Supporting Information for The Disproportionate Role of Ocean Topography on the Upwelling of Carbon in the Southern Ocean

Riley X. Brady[1], Mathew E. Maltrud[2], Phillip J. Wolfram[2], Henri F. Drake[3],

and Nicole S. Lovenduski[1]

[1]Department of Atmospheric and Oceanic Sciences and Institute of Arctic and Alpine Research, University of Colorado, Boulder, CO, USA

[2]Fluid Dynamics and Solid Mechanics (T-3), Los Alamos National Laboratory, Los Alamos, NM, USA

[3]MIT-WHOI Joint Program in Oceanography/Applied Ocean Science & Engineering, Cambridge and Woods Hole, MA, USA

Contents of this file

1. Text S1 to S2
2. Figures S1 to S5

Additional Supporting Information (Files uploaded separately)

1. Caption for Movie S1

Introduction The supporting information serves to provide a more detailed description of the Eulerian model configuration and to evaluate its performance against observations. We show the Eulerian model mesh resolution via a snapshot of dissolved inorganic carbon in the Drake Passage in Figure S1 and as a function of latitude in Figure S2. In Text S1, we describe the use of (or lack thereof) subgrid-scale parameterizations, detail the ocean biogeochemical model, and outline the initialization and spinup strategy. In Text S2, we assess the Eulerian model's fidelity at simulating horizontal transport in the Antarctic Circumpolar Current (Figure S3), mixed layer depths (Figure S4), and deep concentrations of dissolved inorganic carbon (Figure S5).

Text S1. As mentioned in the main text, we use the ocean and sea ice components of the Energy Exascale Earth System Model (E3SM) in this study (Burrows et al., 2020), the Model for Prediction Across Scales Ocean (MPAS-O) and SeaIce (Ringler et al., 2013). Due to the high resolution of the horizontal mesh (Figure S1 and S2), we resolve mesoscale eddies and thus do not parameterize the effect of baroclinic instabilities on horizontal tracer diffusion. However, we do parameterize the effect of vertical mixing on tracer distributions using the K-profile parameterization (KPP; Large, McWilliams, and Doney (1994)).

The ocean biogeochemical component is derived from the Biogeochemical Elemental Cycling (BEC) model, which contains three phytoplankton functional types (diatoms, diazotrophs, and a small calcifying phytoplankton class), a single zooplankton class, seawater carbonate chemistry, and also tracks the cycling of C, N, P, Fe, Si, and O (Moore et al., 2013). MPAS-O adds additional features to BEC, including prognostic dimethyl sulfide (DMS) production and an explicit *Phaeocystis* phytoplankton class (Wang & Moore, 2011).

Prior to initializing the biogeochemical model, we spun up the ocean and sea ice models from rest for 25 years with CORE-II interannual forcing. We then initialized the ocean biogeochemistry using climatologies from observationally based data products. DIC and alkalinity were initialized using pre-industrial values from the Global Ocean Data Analysis Project (GLODAP; Key et al. (2004)), and nutrients were initialized using the *World Ocean Atlas* (WOA; Garcia et al. (2013)). The physical and biogeochemical models were then spun up for 33 years to reach approximate steady-state in air-sea CO_2 fluxes in the Southern Ocean (not shown). After the spinup, the global integral of air-sea CO_2 flux has a relatively small linear drift of 0.05 PgC yr^{-2}.

Text S2. Here, we provide further evaluation of the MPAS-O simulation, focusing on horizontal transport in the ACC, mixed layer depth, and deep concentrations of DIC. We first compare the barotropic stream function (BSF) in MPAS-O to a high resolution state estimate of the Southern Ocean (Mazloff et al., 2010) in Figure S3. We find general agreement between our simulation and the state estimate, with cyclonic polar gyres in the Ross and Weddell Seas, and similar magnitudes and locations for ACC streamlines (Figure S3). Next, we assess the annual mean mixed layer depth against Argo-based observations from Holte, Talley, Gilson, and Roemmich (2017) (Figure S4). Our model reproduces the spatial patterns of the observational product, with deeper mixed layers in the ACC downstream of the Kerguelan Plateau and in the Pacific sector (Figure S4). Within the ACC (south of 45^oS and outside of the annual sea ice zone), we find a pattern correlation of 0.72 with the observational product and a mean absolute error (MAE) of 21 m. Note that our model does have very deep mixed layers within the sea-ice zone due to open-ocean polynyas (not shown), which has been documented in other ocean models (Zanowski et al., 2015). While this is unlikely to affect the results of our study, it could have an impact on tracer distributions in the Southern Ocean. Lastly, we evaluate the deep-water stores of pre-industrial DIC in our model (Figure S5). We find that MPAS-O replicates the broad-scale patterns of the observations well. MPAS-O simulates enriched stores of pre-industrial DIC within the ACC (where curl-driven upwelling occurs) and depleted pre-industrial DIC concentrations equatorward of the ACC (Figure S5). This results in a pattern correlation of 0.90 within the ACC and an MAE of 14 μmol kg^{-1}. Note that the model simulates slightly lower levels of pre-industrial DIC at depth in the ACC than observations, and thus our results likely underestimate carbon upwelling along particle trajectories.

Movie S1. Lagrangian flow of dissolved inorganic carbon (DIC) in the Southern Ocean between 300 m and 2000 m for an arbitrary year of the simulation. Output is stored and visualized in two day increments, with the previous week's history drawn to outline mesoscale eddy activity. Pathlines are colored by the instantaneous DIC recorded by the particle at model runtime.

References

Burrows, S., Maltrud, M., Yang, X., Zhu, Q., Jeffery, N., Shi, X., ... others (2020). The DOE E3SM v1. 1 biogeochemistry configuration: description and simulated ecosystem-climate responses to historical changes in forcing. *Journal of Advances in Modeling Earth Systems*, e2019MS001766.

Garcia, H. E., Locarnini, R. A., Boyer, T. P., Antonov, J. I., Baranova, O. K., Zweng, M. M., ... Levitus, S. (2013). World Ocean Atlas 2013. volume 4, dissolved inorganic nutrients (phosphate, nitrate, silicate).

Holte, J., Talley, L. D., Gilson, J., & Roemmich, D. (2017). An argo mixed layer climatology and database. *Geophysical Research Letters*, *44*(11), 5618–5626.

Key, R. M., Kozyr, A., Sabine, C. L., Lee, K., Wanninkhof, R., Bullister, J. L., ... Peng, T.-H. (2004). A global ocean carbon climatology: Results from Global Data Analysis Project (GLODAP). *Global biogeochemical cycles*, *18*(4).

Large, W. G., McWilliams, J. C., & Doney, S. C. (1994). Oceanic vertical mixing: A review and a model with a nonlocal boundary layer parameterization. *Reviews of Geophysics*, *32*(4), 363–403.

Mazloff, M. R., Heimbach, P., & Wunsch, C. (2010). An eddy-permitting Southern Ocean state estimate. *Journal of Physical Oceanography*, *40*(5), 880–899.

Moore, J. K., Lindsay, K., Doney, S. C., Long, M. C., & Misumi, K. (2013). Marine ecosystem dynamics and biogeochemical cycling in the Community Earth System Model [CESM1 (BGC)]: Comparison of the 1990s with the 2090s under the RCP4.5 and RCP8.5 scenarios. *Journal of Climate*, *26*(23), 9291–9312.

Ringler, T., Petersen, M., Higdon, R. L., Jacobsen, D., Jones, P. W., & Maltrud, M. (2013). A multi-resolution approach to global ocean modeling. *Ocean Modelling*, *69*, 211–232.

Wang, S., & Moore, J. K. (2011). Incorporating Phaeocystis into a Southern Ocean ecosystem model. *Journal of Geophysical Research: Oceans*, *116*(C1).

Zanowski, H., Hallberg, R., & Sarmiento, J. L. (2015). Abyssal ocean warming and salinification after Weddell polynyas in the GFDL CM2G coupled climate model. *Journal of Physical Oceanography*, *45*(11), 2755–2772.

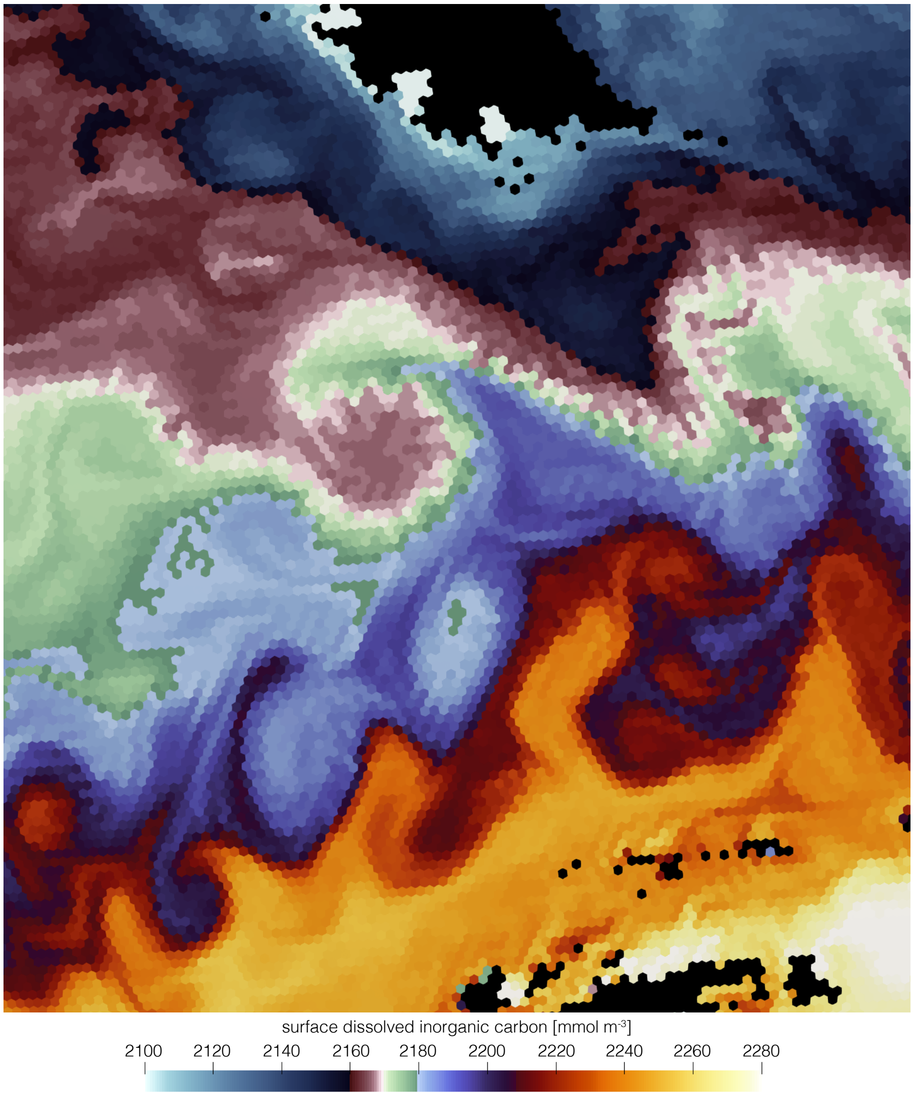

Figure S1. A snapshot of an arbitrary five-day average surface dissolved inorganic carbon (DIC) field in December. This showcases DIC levels in the Drake Passage, where black grid cells outline the southern tip of South America (top) and northern extent of the Antarctic Peninsula (bottom). Hexagonal pixels show the actual Eulerian mesh and its horizontal resolution, which is approximately 14.5 km in this region (Figure S2).

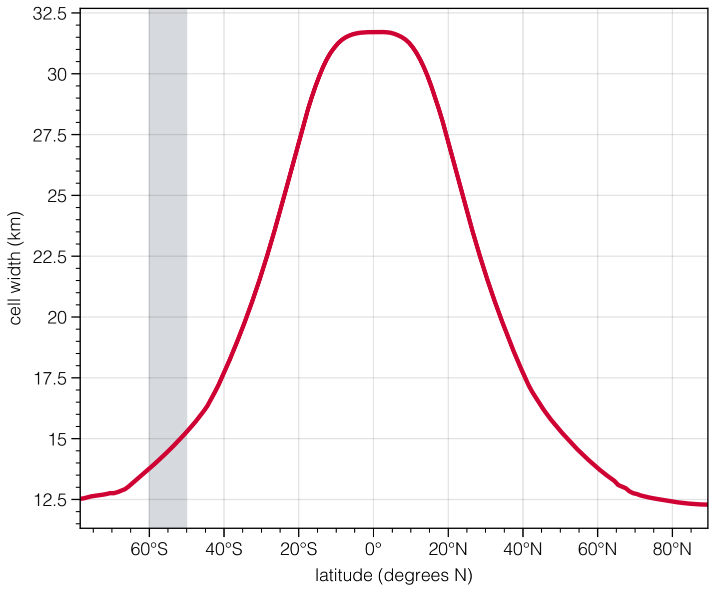

Figure S2. Horizontal resolution of grid cells for the ocean model used in this study. The average hexagonal width of the Model for Prediction Across Scales-Ocean (MPAS-O) are shown as a function of latitude, with the approximate extent of the Antarctic Circumpolar Current (50^oS–60^oS shaded in gray).

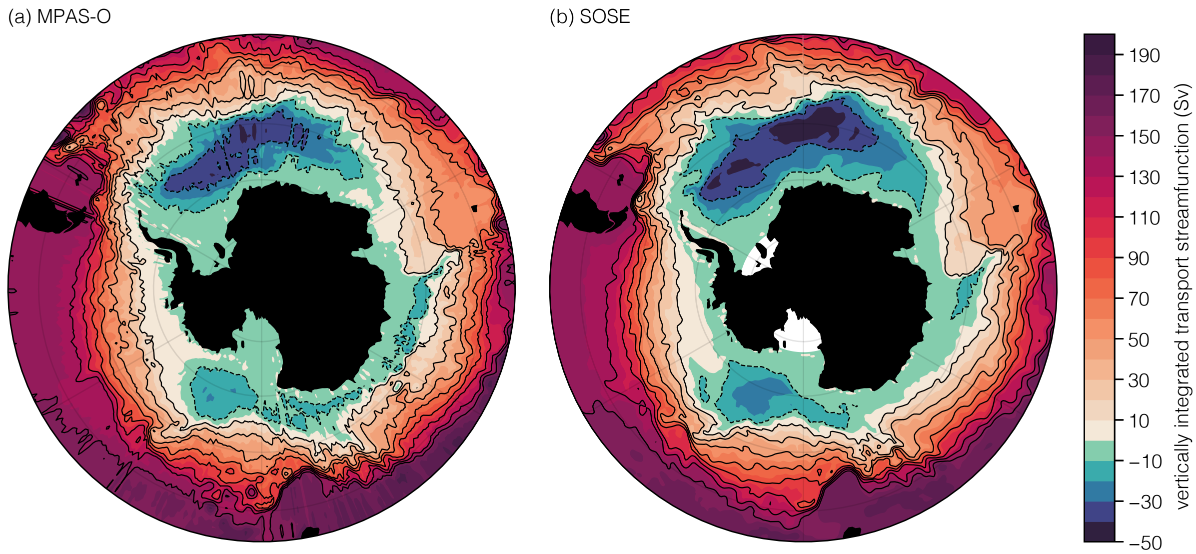

Figure S3. Model evaluation of the vertically integrated horizontal transport streamfunction. (a) Annual climatology of the barotropic streamfunction for the Model for Prediction Across Scales–Ocean (MPAS-O), the model used in this study. (b) Barotropic streamfunction for a solution of the Southern Ocean State Estimate (SOSE; Mazloff et al. (2010)). Contours outline 20 Sv increments. The model's climatology for 75% annual sea ice extent is outlined in black and mixed layer depths are not compared within this region to focus on the Antarctic Circumpolar Current.

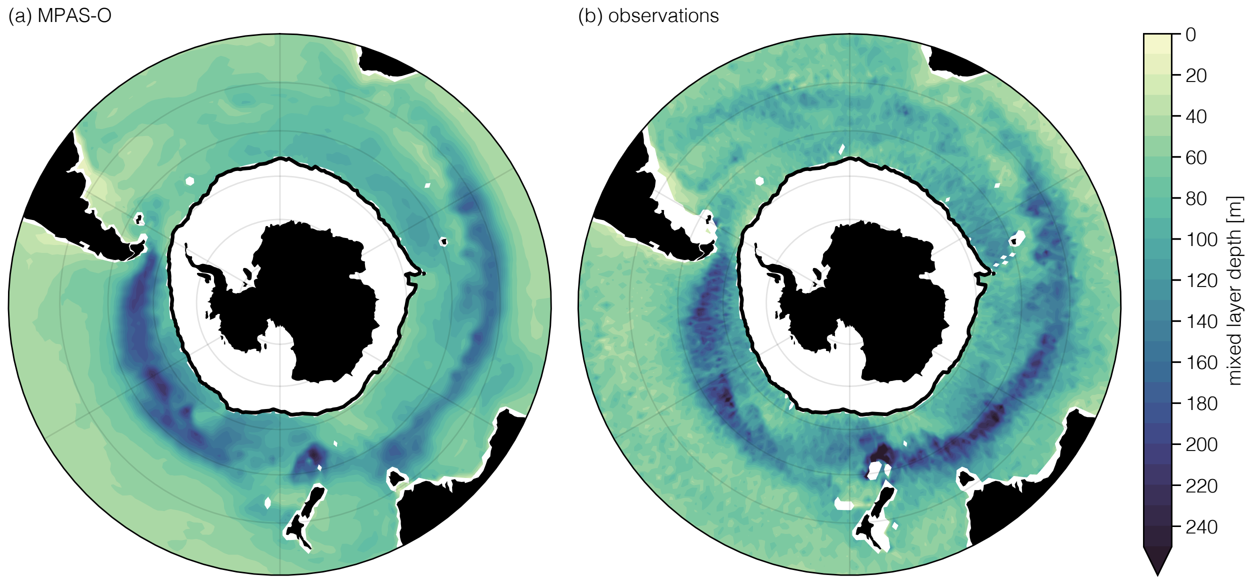

Figure S4. Model evaluation of annual mixed layer depth. (a) Annual climatology for mixed layer depth for the Model for Prediction Across Scales–Ocean (MPAS-O), the model used in this study. (b) Annual mean mixed layer depth from Holte et al. (2017)'s ARGO-based observational climatology. The model's climatology for 75% annual sea ice extent is outlined in black and mixed layer depths are not compared within this region to focus on the Antarctic Circumpolar Current.

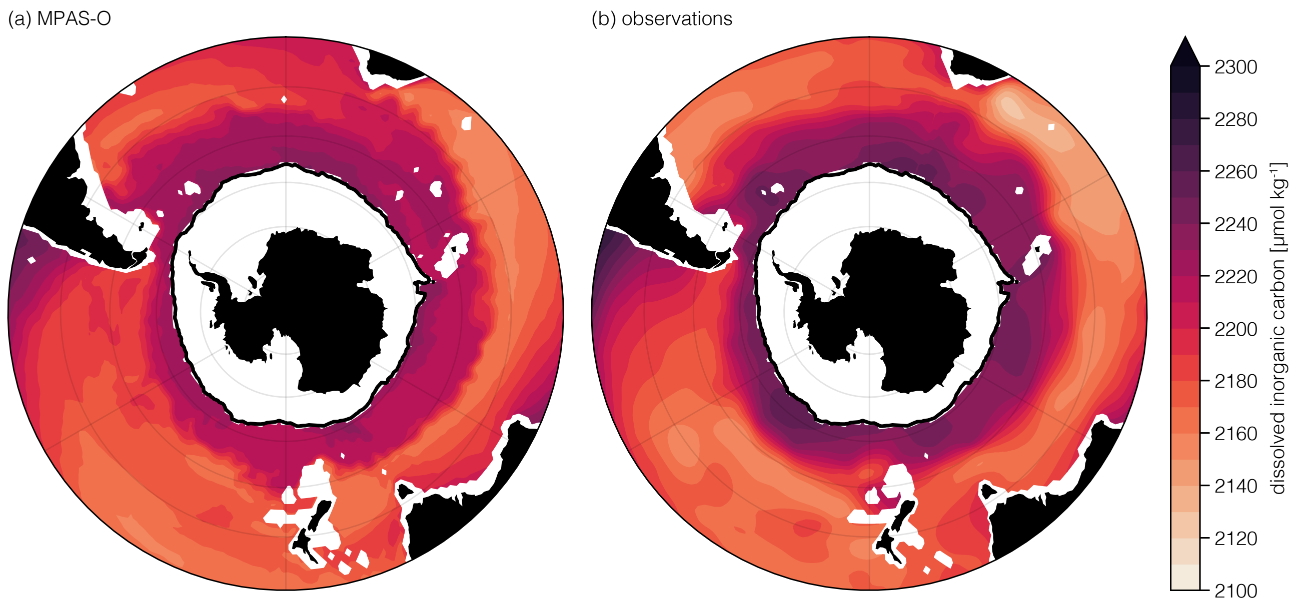

Figure S5. Model evaluation of dissolved inorganic carbon (DIC) at 1000 m. (a) Annual climatology for DIC at 1000 m for the Model for Prediction Across Scales–Ocean (MPAS-O), the model used in this study. (b) Annual mean pre-industrial DIC from the Global Ocean Data Analysis Project (GLODAP; Key et al. (2004)). The model was compared to the pre-industrial DIC observational product, since that is what was used to initialize the simulation. The model's climatology for 75% annual sea ice extent is outlined in black.